BJR

https://doi.org/10.1259/bjr.20201047

Received: 29 August 2020 | Revised: 01 December 2020 | Accepted: 09 December 2020

Cite this article as:
Zhan C, Chen Q, Zhang M, Xiang Y, Chen J, Zhu D, et al. Radiomics for intracerebral hemorrhage: are all small hematomas benign?. *Br J Radiol* 2021; **94**: 20201047.

FULL PAPER

Radiomics for intracerebral hemorrhage: are all small hematomas benign?

CHENYI ZHAN, MD, QIAN CHEN, MD, MINGYUE ZHANG, MD, YILAN XIANG, MD, JIE CHEN, MD, DONGQIN ZHU, MD, CHAO CHEN, MD, TIANYI XIA, MD and YUNJUN YANG, MD, PhD

Department of Radiology, The First Affiliated Hospital of Wenzhou Medical University, Wenzhou, China

Address correspondence to: Dr Yunjun Yang
E-mail: *yyjunjim@163.com*

Objectives: We hypothesized that not all small hematomas are benign and that radiomics could predict hematoma expansion (HE) and short-term outcomes in small hematomas.
Methods: We analyzed 313 patients with small (<10 ml) intracerebral hemorrhage (ICH) who underwent baseline non-contrast CT within 6 h of symptom onset between September 2013 and February 2019. Poor outcome was defined as a Glasgow Outcome Scale score ≤3. A radiomic model and a clinical model were built using least absolute shrinkageand selection operator algorithm or multivariate analysis. A combined model that incorporated the developed radiomic score and clinical factors was then constructed. The area under the receiver operating characteristic curve (AUC) was used to evaluate the performance of these models.
Results: The addition of radiomics to clinical factors significantly improved the prediction performance of HE compared with the clinical model alone in both the training {AUC, 0.762 [95% CI (0.665–0.859)] versus AUC, 0.651 [95% CI (0.556–0.745)], p = 0.007} and test {AUC, 0.776 [95% CI (0.655–0.897) versus AUC, 0.631 [95% CI (0.451–0.810)], p = 0.001} cohorts. Moreover, the radiomic-based model achieved good discrimination ability of poor outcomes in the 3–10 ml group (AUCs 0.720 and 0.701).
Conclusion: Compared with clinical information alone, combined model had greater potential for discriminating between benign and malignant course in patients with small ICH, particularly 3–10 ml hematomas.
Advances in knowledge: Radiomics can be used as a supplement to conventional medical imaging, improving clinical decision-making and facilitating personalized treatment in small ICH.

INTRODUCTION

Intracerebral hemorrhage (ICH) is the most devastating subtype of stroke with high morbidity and mortality.[1] Baseline hematoma volume is an independent predictor of hematoma expansion (HE) and poor outcome in patients with ICH.[2,3] Although patients with smaller hematomas are more likely to have a benign clinical course,[4,5] some studies reported that small hemorrhage in deep locations caused functional dependence or mortality, and the volume cut-off to predict poor outcome was less than the widely used of 30 ml.[6–8] In a prior study, small ICH was defined as benign or malignant, and patients with the latter experienced HE and had worse outcomes.[5]

Several clinical trials have also enrolled many patients with small-volume ICH,[9–11] but these trials failed to demonstrate a clinical benefit of the intervention. One possibility might be that small ICH is malignant in only a proportion of patients and those with benign small ICH have little opportunity to benefit from treatment. Therefore, it is important to improve patient selection and identify those with malignant small hematomas at high risk of expansion. Currently, there is no standard definition of small hematoma.[4,5,12,13] As the average ICH volume in clinical trials is approximately10 ml, we defined small hematomas as those with a baseline hematoma volume less than 10 ml.

Radiomics is an emerging approach that extracts high-throughput quantitative features from medical images and enables us to utilize the full potential of images.[14,15] It has been widely used for the prediction of cancer and differentiation of benign and malignant tumors.[16,17] Recently, radiomic analyses have been applied to ICH for the prediction of HE.[18–20] However, clinical risk factors known to be associated with HE were not taken into account in these studies. Moreover, to the best of our knowledge, no study has applied radiomics to

predict HE or the short-term outcomes in patients with small hematomas.

Therefore, in this study, we hypothesized that not all small hematomas (<10 ml) are benign and that radiomics could predict HE and the short-term outcomes in patients with small hematomas. The first aim of this study was to train a radiomic score (R-score) to predict HE in patients with small ICH. The second aim was to assess the applicability of the same R-score to the prediction of HE and the short-term outcomes in the 3–10 ml and <3 ml subgroup. The last aim was to train a new radiomic score (Rad-score) to predict the short-term outcomes in patients with volumes of 3–10 ml.

METHODS AND MATERIALS

Study design and patient population

We retrospectively analyzed the records of patients aged >18 years who presented with primary ICH at our Neurological Emergency Room between September 2013 and February 2019. The inclusion criteria were as follows: (1) a baseline noncontrast computed tomography (NCCT) scan performed within 6 h after symptom onset; (2) a follow-up NCCT scan performed within 72 h after the initial CT scan; and (3) Glasgow Outcome Scale (GOS) score evaluated at discharge. The exclusion criteria were as follows: (1) secondary ICH (tumor, trauma, cerebral aneurysm, arteriovenous malformation, or hemorrhagic transformation from brain infarction); (2) primary intraventricular hemorrhage (IVH) or multiple cerebral hemorrhage; (3) surgical evacuation before the follow-up NCCT scan; (4) anticoagulant-associated ICH; and (5) CT images with severe motion artifacts.

Patients were randomly assigned to the training or test cohorts. HE was defined as a relative increase of 33% or an absolute increase of 6 ml of a hematoma from the baseline volume.[21] Poor outcome was defined as a GOS score ≤3 at discharge.[22–24]

The requirement for written informed consent was waived owing to the retrospective design of the study.

Image acquisition and segmentation

All patients were examined using a 64-slice spiral CT scanner (LightspeedVCT64; GE Medical Systems, Milwaukee, WI). The baseline and follow-up CT scans were performed using a standard clinical protocol with an axial technique, with slice thickness of 5 mm, tube voltage of 120 kV(p), and tube current of 80 mA.

Figure 1 illustrated the flow chart of the study. All images were analyzed by a radiologist (2-year experience) blinded to the patients' identity and clinical data. The contours of all intracerebral hematomas were drawn manually layer-by-layer. 50 images were randomly chosen and were assessed by another radiologist (5-year experience). The ventricular extension was not included. Three-dimensional segmentation of the region of interest (ROI) was performed using the ITK-SNAP software (v. 3.8, www.itksnap.org) (Figure 2).

Clinical analysis

The essential clinical data, including age, sex, history of hypertension, diabetes mellitus, ischemic stroke, ICH, and Glasgow coma scale (GCS) scores, were recorded after admission. We also recorded the time from symptom onset to CT, location of the hematoma [deep (basal ganglia, thalamus), other (lobar, cerebellum, brainstem)], presence of IVH, and hematoma volume after the initial NCCT scan. Two radiologists (2 year and 5 year experience) blinded to the patients' identity and clinical data interpreted the baseline NCCT images to assess the following features: (1) satellite sign ;(2) black hole sign ;(3) blend sign; and (4) Island sign. In case of discrepancy, the final decisions were reached by consensus.

Radiomic analysis

In our study, the set of radiomic features contained 396 descriptors from 5 groups: (1) first-order statistics of intensity (n = 42) (2) shape (n = 20) (3) gray-level co-occurrence matrix (n = 144) (4) gray-level run length matrix (n = 172), and (5) Haralick features (n = 18). Feature extraction was performed using the Artificial Intelligence Kit v. 3.0.0..R in the training cohort.

Least absolute shrinkage and selection operator (LASSO) logistic regression was used for feature selection to reduce redundancy. 10-fold cross-validation was applied to choose the tuning parameter that determined the magnitude of penalization. Features with non-zero coefficients were selected to calculate the radiomic score using the following formula:

$$\text{radiomic score} = \sum \beta \text{iXi} + \text{Intercept}(\text{i} = 0, 1, 2, 3), \quad (1)$$

where Xi represents the ith selected radiomic features, and βi is the respective coefficient determined by LASSO regression. We further validated the R-score in subgroups with volumes 3–10 ml and less than 3 ml. Receiver operating characteristic (ROC) curve analysis was performed to assess the predictive performance with the associated classification measures. The Youden index (sensitivity+ specificity-1) was used to select the cut-off value to determine the corresponding sensitivity and specificity. The reproducibility of the radiomic features was assessed using the interclass correlation coefficient (ICC), with an ICC greater than 0.75 indicating good interobserver agreement.

Development and validation of clinical model and combined model

Radiological and clinical characteristics were compared between HE and non-HE (NHE) groups.Predictors of HE with statistical significance in the univariate analysis were introduced into the stepwise multivariate logistic regression analysis to build the clinical model. The identical multivariable regression formula was used to calculate the predictive probability of HE in the test cohort. A combined model that incorporated the developed R-score and clinical model was built using multivariate logistic regression analysis (Supplementary Table 1) in the training cohort and validated in the test cohort.

Figure 1. Flow chart of the study. 3D, three-dimensional; ICH, intracerebralhemorrhage; LASSO, least absolute shrinkageand selection operator; ROI, region of interest.

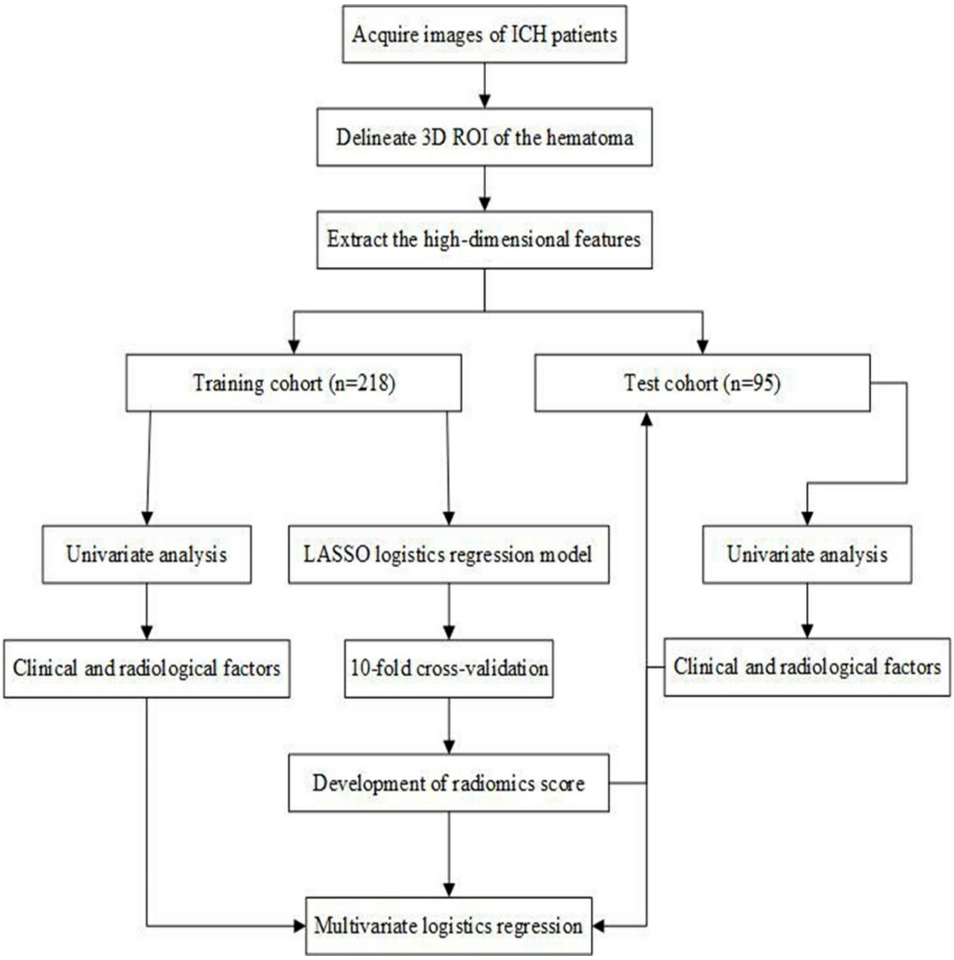

Evaluation of the clinical outcome at discharge

Univariate analysis was used for comparing the differences between patients with favorable (GOS score4–5) and those with poor outcome (GOS score1–3). Multivariate logistic regression analysis with a backward step-wise selection was performed to determine the independent predictors.

Statistical analysis

For categorical variables, differences were calculated using the χ^2 test or Fisher's exact test. Student's *t*-test or Mann–Whitney's *U* test was used for estimating the differences in continuous variables. Normally distributed continuous data were represented as mean ± standard deviation, otherwise as median with interquartile range (IQR). Univariate analysis was used to compare the variables to discover the possible significant predictors for HE and poor outcome. Variables with $p < 0.05$ were included in the multivariate logistic regression analysis. The relative risk was estimated by odds ratios (ORs) with 95% confidence intervals (CIs) for each independent variable. The performance of prediction models was evaluated by plotting the ROC curves and calculating the area under the curve (AUC) values. AUC values were compared between models by using Delong's test. All statistical analyses were performed with SPSS (v 22.0, IBM Corp.,Armonk, New York, USA) and R statistical software (v. 3.6.1,https://www.r-project.org). A two-sided p value < 0.05 was considered statistically significant.

RESULTS

Patients' characteristics

In total, 313 patients with ICH were included in the final analysis. There were 218 patients in the training cohort and 95 in the test cohort.

The baseline characteristics of the training and test cohorts are detailed in Table 1. The characteristics of the subgroups are presented in Tables 2 and 3.The incidence of HE was 13.8% (30 of 218) in the training cohort and 14.7% (14 of 95) in the test cohort. No significant difference was found between the two cohorts (all $p > 0.05$). In the subgroup analysis, HE was observed in 28 patients (11.2%) of the 3–10 ml subgroup and in 16 patients (25.8%) of the <3 ml subgroup.

Development and validation of the radiomic score

After evaluating the differentiating ability of the radiomic features in the univariate analysis, 58 features with p values <0.05 were selected. These features were reduced to three

Figure 2. Manual 3D segmentation of the hematoma. (a) The patient's baseline CT showed a small hematoma in the left basal ganglia (58 years, male, baseline volume = 7.41 ml, radiomic score = −1.145). (b) Delineation of the lesion using the ITK-SNAP software. (c) Generation of a 3D region of interest. (d) Detection of hematoma expansion on follow-up CT (volume = 16.92 ml, Glasgow outcome scale score = 3). 3D, three-dimensional.

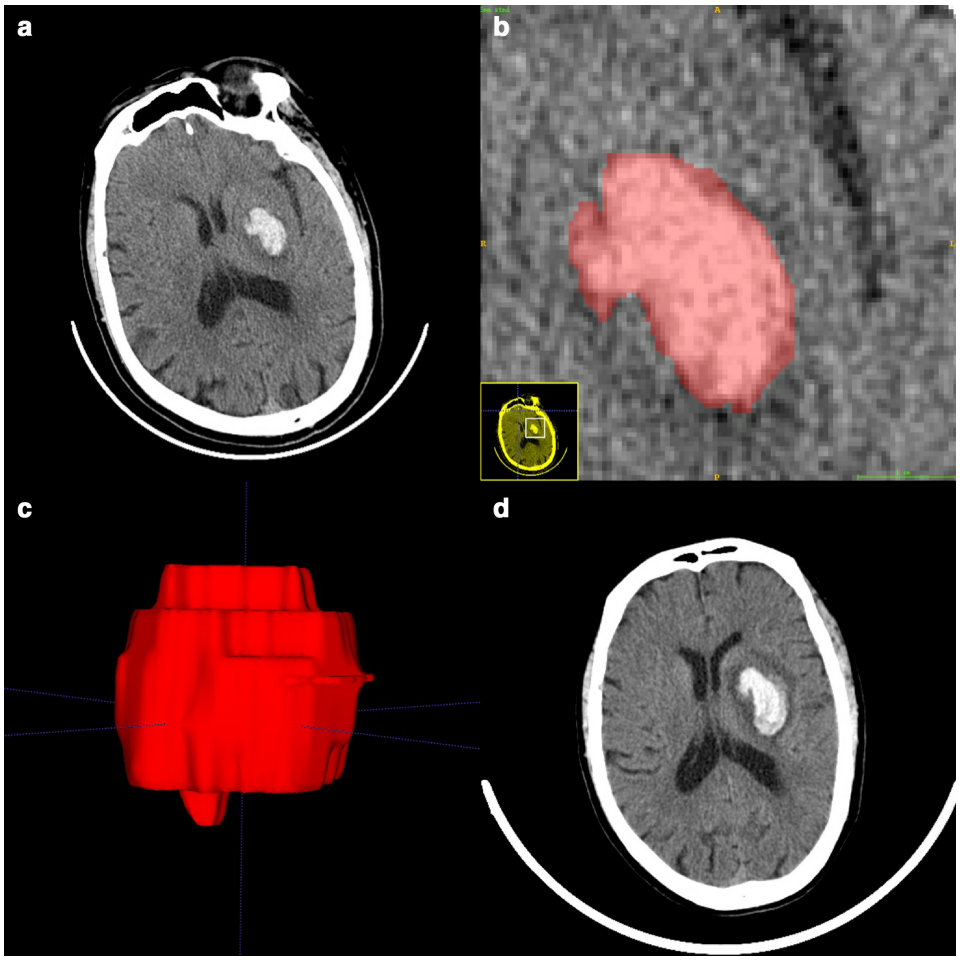

potential predictors (kurtosis, HaralickCorrelation_AllDirection_offset1_SD, ShortRunHighGreyLevelEmphasis_AllDirection_offset4_SD) that had non-zero coefficients in the LASSO logistic regression model in the training cohort (Figure 3). The R-score was then calculated using the following formula:

$$\begin{aligned} R-score = {} & -2.180 - 0.299 \times kurtosis - 0.858 \times \\ & HaralickCorrelation\_AllDirection\_offset1\_SD - 0.272 \times \\ & ShortRunHighGreyLevelEmphasis\_AllDirection\_offset4\_SD. \end{aligned} \quad (2)$$

R-score = −2.180–0.299 × kurtosis - 0.858 × HaralickCorrelation_AllDirection_offset1_SD - 0.272 × ShortRunHighGreyLevelEmphasis_AllDirection_offset4_SD. (2)

The calculated R-scores are summarized in Table 1. There were significant differences between the HE and non-HE (NHE) groups in the training and test cohorts, and the 3–10 ml subgroup (all $p < 0.001$; Tables 1 and 2). A new radiomic score (Rad-score) for predicting the short-term outcome was established using the same flow. The calculated Rad-scores are summarized in Supplementary Table 2.

Association between the radiomics and HE

Multivariate logistic regression analysis indicated the R-score as an independent predictor of HE in the training cohort [OR, 2.557; 95% CI (1.455–4.492); $p = 0.001$] and the test cohort [OR, 3.898; 95% CI (1.051–14.453); $p = 0.042$] (Table 4).

In the 3–10 ml subgroup, patients with HE had higher R-scores (Table 2) and the R-score was independently associated with HE [OR, 4.293; 95% CI (2.095–8.796); $p < 0.001$)] after adjusting for confounders (Table 5). In the <3 ml subgroup, univariate analysis showed that there was no significant difference in the R-score between the HE and NHE groups (Table 3).

The performance of three prediction models the radiomic model, the clinical model, and the combined model was summarized in Table 6. AUCs of three prediction models were shown in Figure 4. In the training cohort, the AUC value of the combined model was 0.762 [95% CI (0.665–0.859)], outperformed the

Table 1. Patients' baseline characteristics

	Training cohort (n = 218)			Test cohort (n = 95)			
	HE (n = 30)	NHE (n = 188)	p value	HE (n = 14)	NHE (n = 81)	p value	p^a -value
Age, y, mean (SD)	64.0 (9.1).	62.6 (12.0)	0.541	56.6 (8.6)	63.1 ± 11.9	0.022	0.657
Male	22 (73.3)	106 (56.4)	0.080	8 (57.1)	46 (56.8)	0.98	0.757
Medical history							
Arterial hypertension	26 (86.7)	159(85)	1	11 (78.6)	69 (88.5)	0.384	0.695
Diabetes mellitus	6 (20)	31 (16.6)	0.644	3 (21.4)	15 (19.2)	1	0.597
ICH	1 (3.3)	8 (4.3)	1	2 (14.3)	3 (3.8)	0.165	0.765
Ischemic stroke	3 (10)	10 (5.3)	0.397	0	6 (7.7)	0.586	0.859
IVH	4 (13.3)	71 (37.8)	0.009	3 (21.4)	29 (35.8)	0.37	0.902
Black hole sign	5 (16.7)	10 (5.3)	0.039	4 (28.6)	2 (2.5)	0.004	0.854
Blend sign	3 (10)	5 (2.7)	0.082	3 (21.4)	3 (3.7)	0.04	0.372
Island sign	2 (6.7)	6 (3.2)	0.303	0	3 (3.7)	1	1
Satellite sign	9 (30)	29 (15.4)	0.051	2 (14.3)	16 (19.8)	1	0.748
Location			0.851			0.084	0.279
Deep	25 (83.3)	154 (81.9)		8 (57.1)	65 (80.2)		
Other	55 (16.7)	34 (18.1)		6 (42.9)	16 (19.8)		
Hematoma volume, ml, mean (SD)	5.3 (3.0)	5.7 (2.6)	0.431	5.8 (3.6)	6.2 (2.5)	0.637	0.204
Time from onset to CT, h, mean (SD)	2.6 (1.4)	3.1 (1.5)	0.073	2.2 (1.3)	3.2 (1.5)	0.02	0.853
Admission GCS score, median (IQR)	14 (10.5–15)	15 (14–15)	0.066	15 (11–15)	15 (12–15)	0.928	0.156
R-score, median (IQR)	−1.257 (−2.055–−0.977)	−2.088 (−2.970–−1.077)	<0.001	−1.461 (−1.810–−1.230)	2.097 (−2.824–1.388)	<0.001	1
Poor outcome	23 (76.7)	87 (46.3)	0.002	10 (71.4)	48 (59.3)	0.389	0.084

GCS, Glasgow coma scale; HE, Hematoma expansion; ICH, Intracerebral hemorrhage; IQR, Interquartile range; IVH, Intraventricular hemorrhage; NHE, Non-hematoma expansion; R-score, Radiomic score; SD, Standard deviation.
All values are presented as count (%) unless otherwise specified.
[a]Indicates comparison between the training and test cohorts.

clinical model (AUC, 0.651 [95% CI, 0.556–0.745], p = 0.007) and was comparable with that of the radiomic model (AUC, 0.728 [95% CI (0.631–0.826)], p = 0.136). Similarly, the combined model showed a better predicting performance than the clinical model alone in the test cohorts {AUC, 0.776 [95% CI (0.655–0.897)] versus AUC, 0.631 [95% CI (0.451–0.810)], p = 0.001}. The AUC value was 0.740 [95% CI (0.659–0.820)] in the 3–10 ml subgroup. Furthermore, the optimal cutoff value for the R-score was −1.430 in the training cohort according to the Youden index. The interobserver agreement on the radiomic features reached a mean ICC of 0.89.

Association between the radiomics and short-term poor outcomes

Of the 313 patients with small ICH, 168 (53.7%) had poor outcomes at discharge. In the two subgroups, 143 (57%) of the 251 patients in the 3–10 ml subgroup and 25 (40.3%) of the 62 patients in the <3 ml subgroup had poor outcomes. The rate of poor outcome was significantly lower in the <3 ml subgroup (40.3% *vs* 57%; p = 0.019).

In the 3–10 ml subgroup, the multivariate logistic regression analysis indicated that the R-score [OR, 1.297; 95% CI (1.004–1.674); p = 0.046] were an independent predictor of poor outcomes (Table 5). In the <3 ml subgroup, the univariate analysis showed no significant difference in the R-score between patients with poor and those with favorable outcome (Table 3). Supplementary Table 2 shows detailed baseline characteristics of patients with poor and favorable outcome in the 3–10 ml group; baseline characteristics did not differ between the derivation and validation cohorts. The radiomics-based model indicated favorable prediction of poor outcomes with a AUC vaule of 0.720 (95% CI: 0.643–0.790) in the derivation cohort and 0.701 [95% CI (0.580–0.822)] in the validation cohort (Supplementary Table 3, Figure 5).

Table 2. Univariate analysis for hematoma expansion and poor outcome in the 3–10 ml subgroup

	HE (n = 251)			Poor outcome (n = 251)		
	HE (n = 28)	NHE (n = 223)	p value	Poor outcome (n = 143)	Favorable outcome (n = 108)	p value
Age, y, mean (SD)	61.3 (10.6)	63.0 (12.1)	0.467	63.7 (11.3)	61.6 (12.7)	0.180
Male	18 (64.3)	126 (56.5)	0.432	77 (53.8)	67 (62.0)	0.201
Arterial hypertension	24 (85.7)	191 (87.2)	0.768	122 (87.8)	93 (86.1)	0.700
Diabetes mellitus	6 (21.4)	37 (16.9)	0.596	25 (18.0)	18 (16.7)	0.786
ICH	1 (3.6)	8 (3.7)	1	4 (2.9)	5 (4.6)	0.510
Ischemic stroke	2 (7.1)	16 (7.3)	1	12 (8.6)	6 (5.6)	0.356
IVH	7 (25)	90 (40.4)	0.116	58 (40.6)	39 (36.1)	0.474
Black hole sign	5 (17.9)	12 (5.4)	0.029	14 (9.8)	3 (2.8)	0.029
Blend sign	4 (14.3)	8 (3.6)	0.033	6 (4.2)	6 (5.6)	0.617
Island sign	2 (7.1)	8 (3.6)	0.309	9 (6.3)	1 (0.9)	0.047
Satellite sign	8 (28.6)	38 (17)	0.137	31 (21.7)	15 (13.9)	0.114
Location			1			0.001
Deep	24 (85.7)	188 (84.3)		130 (90.9)	82 (75.9)	
Other	4 (14.3)	35 (15.7)		13 (9.1)	26 (24.1)	
Hematoma volume, ml, mean (SD)	7.5 (1.9)	6.7 (2.0)	0.034	6.8 (2.0)	6.7 (2.0)	0.699
Time from onset to CT, h, mean (SD)	2.5 (1.4)	3.1 (1.5)	0.055	2.9 (1.4)	3.2 (1.5)	0.170
Admission GCS score, median (IQR)	14(9–15)	15 (13–15)	0.009	14 (11–15)	15 (15–15)	<0.001
R-score, median (IQR)	−1.391 (−1.932–−1.108)	−2.247 (−3.114–−1.421)	<0.001	−1.968 (−2.749–−1.288)	−2.382 (−3.257–−1.427)	0.024

GCS, Glasgow coma scale; HE, Hematoma expansion; ICH, Intracerebral hemorrhage; IQR, Interquartile range; IVH, Intraventricular hemorrhage; NHE, Non-hematoma expansion; R-score, Radiomic score; SD, Standard deviation.

All values are presented as count (%), unless otherwise specified.

Table 3. Univariate analysis for hematoma expansion and poor outcome in the <3 ml subgroup

	HE (n = 62)			Poor outcome (n = 62)		
	HE (n = 16)	NHE (n = 46)	p value	Poor outcome (n = 25)	Favorable outcome (n = 37)	p value
Age, y, mean (SD)	62.3 (7.6)	61.4 (10.8)	0.771	63.8 (7.7)	60.1 (11.2)	0.160
Male	12(75)	26 (56.5)	0.191	16 (64.0)	22 (59.5)	0.719
Arterial hypertension	13 (81.3)	37 (80.4)	1	18 (72.0)	32 (86.5)	0.198
Diabetes mellitus	3 (18.8)	9 (19.6)	1	4 (16.0)	8 (21.6)	0.747
ICH	2 (12.5)	3 (6.5)	0.597	4 (16.0)	1 (2.7)	0.148
Ischemic stroke	1 (6.3)	0	0.258	1 (4.0)	0	0.403
IVH	0	10 (21.7)	0.052	1 (4.0)	9 (24.3)	0.040
Blackhole sign	4 (25)	0	0.003	3 (12.0)	1 (2.7)	0.294
Blend sign	2 (12.5)	0	0.063	2 (8.0)	0	0.159
Island sign	0	1 (2.2)	1	0	1 (2.7)	1
Satellite sign	3 (18.8)	7 (15.2)	0.709	7 (28.0)	3 (8.1)	0.074
Location			0.422			0.311
Deep	9 (56.0)	31 (67.4)		18 (72.0)	22 (59.5)	
Other	7 (44.0)	15 (32.6)		7 (28.0)	15 (40.5)	
Hematoma volume, ml, mean (SD)	1.9 (0.7)	1.8 (0.7)	0.848	2.2 (0.5)	1.6 (0.7)	0.001
Time from onset to CT, h, mean (SD)	2.3 (1.1)	3.2 (1.3)	0.030	3.0 (1.3)	2.9 (1.3)	0.890
Admission GCS score, mean (SD)	14 (3)	14 (2)	0.980	13 (3)	14 (2)	0.039
R-score, mean (SD)	−1.603 (0.865)	−1.963 (0.834)	0.146	−1.780 (0.844)	−1.931 (0.860)	0.498

GCS, Glasgow coma scale; HE, Hematoma expansion; ICH, Intracerebral hemorrhage; IVH, Intraventricular hemorrhage; NHE, Non-hematoma expansion; R-score, Radiomic score; SD, Standard deviation.
All values are presented as count (%), unless otherwise specified.

Figure 3. Radiomic feature selection using the LASSO regression model. We used 10-fold cross-validation to tune parameter (λ) selection in the LASSO model. (a) AUC was plotted *vs* log(λ). Three features with non-zero coefficients were selected using the minimum criteria. (b) LASSO coefficient profiles of the features. Each colored line represents the coefficient of each feature. AUC, area under thecurve; LASSO, least absolute shrinkage and selection operator.

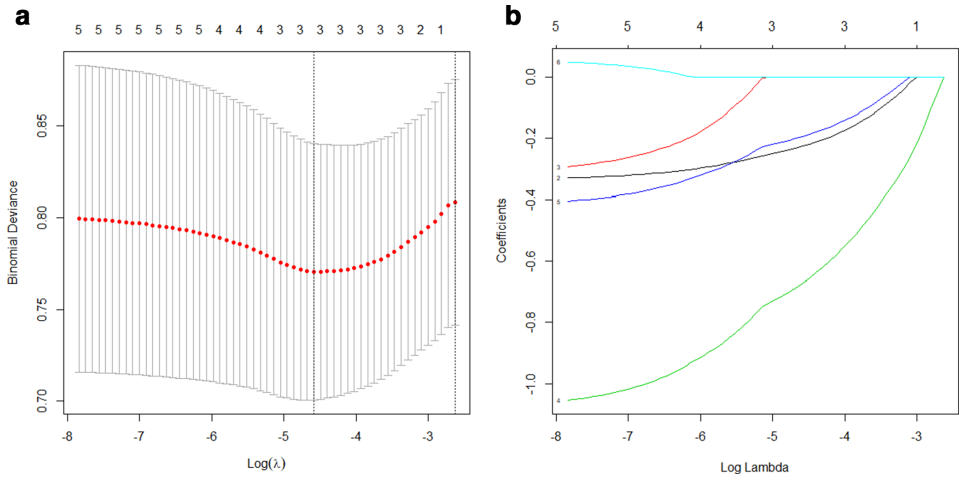

Table 4. Multivariate analysis for hematoma expansion in the training and test cohorts

Variables	Training cohort		Test cohort	
	OR (95% CI)	*p* value	OR (95% CI)	*p* value
IVH	0.292 (0.096–0.890)	0.030	NA	NA
R-score	2.557 (1.455–4.492)	0.001	3.898 (1.051–14.453)	0.042
Black hole sign	2.710 (0.759–9.677)	0.125	10.326 (1.330–80.186)	0.026
Blend sign	NA	NA	3.985 (0.332–47.897)	0.276
Age	NA	NA	0.930 (0.869–0.996)	0.037
Time from onset to CT	NA	NA	0.557 (0.307–1.011)	0.054

CI, Confidence interval; IVH, Intraventricular hemorrhage; NA, Not available;OR, Odds ratio; R-score, Radiomic score.

DISCUSSION

In this retrospective study, we used radiomic anlysis to predict HE and short-term poor outcomes in small hematomas (<10 ml). Combined the radiomic score and the clinical model are superior to the clinical model alone in predicting HE. Our results indicated that small hematomas could exhibit a malignant course and that the R-score based on NCCT was strongly associated with HE. We also found that the radiomic-based model provided good performance of predicting poor outcomes in small hematomas with a volume of 3–10 ml.

To date, most trial inclusion criteria and clinical grading scales have used a cut-off of 30 ml to identify patients likely to have a malignant clinical course with a high expansion rate and a poor outcome.[3,24,25] However, hematomas less than 10 ml could account for approximately one-third to one-half of all patients with ICH[5,13,26] and their destructive effects should not be underestimated. One study demonstrated that baseline hematoma size categories of <10 ml had the same ability to predict outcome regardless of the HE definition.[21] Ironside et al modified the original ICH score and the volume cut-off was less than 10 ml in the deep and brainstem location.[8] Therefore, it is meaningful to discriminate hematomas with a benign clinical course from those with a malignant course so the effects of interventions could be improved. Our results showed that very small hematomas (<3 ml) had a higher rate of HE compared to those with a volume of 3–10 ml, but with a more benign outcome. We further confirmed the findings of other studies that demonstrated very small hematomas were likely to have benign outcomes.[12,13] This may indicate that the very small growth in very small hematomas is insufficient to translate into functional deterioration and the benefits of anti-expansion therapy in those patients may be outweighed by the potential of harm.

Recently, several radiographic features have been used to predict HE and poor outcome, including the black hole sign, blend sign, satellite sign, and CT angiography (CTA) spot sign.[27,28] Li et al[5] reported that patients with benign ICH who had none of these signs would not experience HE. Their definition was complicated for inexperienced radiologists and clinical physicians to make accurate and fast identification. Our R-score could objectively identify patients with HE whose NCCT signs were negative. In the Antihypertensive Treatment of Acute Cerebral Hemorrhage II (ATACH-II) trial, there was no evidence that patients with ICH with CTA spot sign or NCCT signs would benefit from intensive blood pressure reduction.[29,30] It is uncertain whether these signs were inadequate to identify the patients most likely to benefit due to their subjective judgment and somewhat overlapped definition. In addition, the CTA spot sign is unsuited in the emergency room, particularly for patients with ICH with kidney insufficiency and contrast agent allergies, because it is time-consuming and requires a contrast injection. Therefore, quantitative NCCT predictors have been sought to identify subtle changes beyond visual assessment.

Radiomics was initially proved to be useful in tumor assessment due to its ability to quantify the heterogeneity of the ROI and was then applied to ICH.[31] Shen et al[20] demonstrated that by using the

Table 5. Multivariate analysis for hematoma expansion and poor outcome in the 3–10 ml subgroup

Variables	Hematoma expansion		Poor outcome	
	OR (95% CI)	*p* value	OR (95% CI)	*p* value
Blend sign	4.748 (1.114–20.246)	0.035	NA	NA
Hematoma volume	1.385 (1.088–1.762)	0.008	NA	NA
Admission GCS score	0.869 (0.765–0.987)	0.031	0.737 (0.643–0.844)	<0.001
R-score	4.293 (2.095–8.796)	<0.001	1.297 (1.004–1.674)	0.046
Location, deep	NA	NA	5.167 (2.104–12.689)	<0.001
Black hole sign	2.311 (0.666–8.021)	0.187	3.460 (0.724–16.546)	0.120
Island sign	NA	NA	3.641 (0.758–17.487)	0.106

CI, Confidence interval; GCS, Glasgow coma scale; NA, Not available;OR, Odds ratio; R-score, Radiomic score.

Table 6. Predictive performance of the prediction models for hematoma expansion in the training cohort and test cohort

	AUC	Sensitivity	Specificity	PPV	NPV	*p* vaule
Training cohort						
Radiomic model	0.728	0.700	0.729	0.292	0.938	Reference
Clinical model	0.651	0.933	0.356	0.188	0.971	0.141
Combined model	0.762	0.667	0.830	0.385	0.940	0.136
Test cohort						
Radiomic model	0.716	0.786	0.642	0.275	0.945	Reference
Clinical model	0.631	0.286	0.975	0.664	0.888	0.304
Combined model	0.776	0.786	0.691	0.249	0.949	0.120

NPV, Negative predictive value; PPV, Positive predictive value.
AUC indicates area under the receiver operating characteristic curve.

Laplacian of the gaussian bandpass filter, NCCT textures could discriminate between HE and NHE. However, only histogram-based features were analyzed in 108 patients with ICH, which limited the comprehensive assessment of hematoma heterogeneity compared with that achievable with radiomic signatures. Subsequently, Ma et al[19] reported that a five-feature-based R-score could independently evaluate the risk for HE with an accuracy of 0.852. Another study also showed that the radiomic model had an accuracy of 0.726 in predicting HE and the AUC value was 0.729.[18] In accordance with these studies, the R-score in our study showed a good capability of predicting HE (with AUCs of 0.716–0.740), except in very small hematomas. This may further prove that very small hematomas are homogenous and would have a benign course. The haralick correlation measures the degree of similarity of the gray level of the image in the row or column direction. The short run high gray level emphasis measures the joint distribution of short run and high gray level. These two quantitative parameters indicated the diversity between patients with HE and without HE on the specific spatial heterogeneity of gray levels within the region of hematoma. A higher positive kurtosis value represents a sharper peak and wider tails in the histogram. Patients with HE had significantly lower kurtosis. Therefore, patients with HE may show a slimmer tail in the histogram and fewer similar frequencies of different gray values than patients without HE. Our findings were consistent with previous studies that selected one or more of these features as optimum feature for radiomic model construction.[32–34] Recently, Xie et al[35] compared the NCCT-based radiomic model with the conventional radiological model in the prediction of HE. Their analysis revealed that the radiomic model was a reliable and objective method for HE prediction and outperformed the radiological model. Our results also confirmed that the radiomic model was comparable with the combined model. After integrating with the R-score, the clinical model achieved a significantly better performance with a larger AUC value than the clinical model alone indicating statistical contribution of the R-score to the combined model construction. Moreover, we found that in the 3–10 ml baseline hematoma volume category, the R-score was not only associated with HE but could independently predict poor outcomes at discharge. It should be more beneficial if the predictor is not only associated with HE but also related to poor outcomes. We further presented an internally validated radiomic-based model for the prediction of poor outcomes in ICH patients with volumes of 3–10

Figure 4. Comparison of receiver operating characteristic curves between the radiomic model, clinical model and the combined model for predicting hematoma expansion in the training (a) and test (b) cohort. AUC, area under the curve; ROC, receiver operating characteristic..

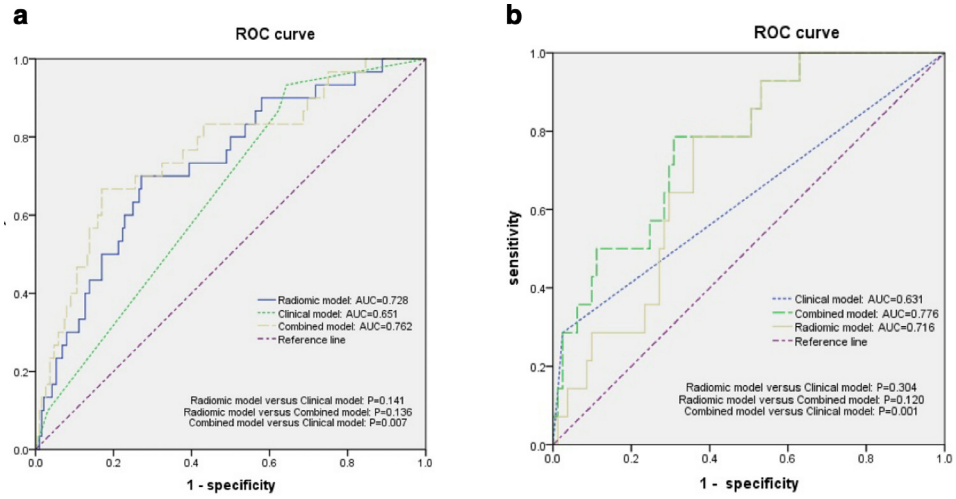

Figure 5. The ROC curves for the radiomic-based models in the derivation (a) and validation(b) cohorts. The area under the curve was 0.720 in the derivation cohort and 0.701 in the validation cohort. ROC, receiver operating characteristic.

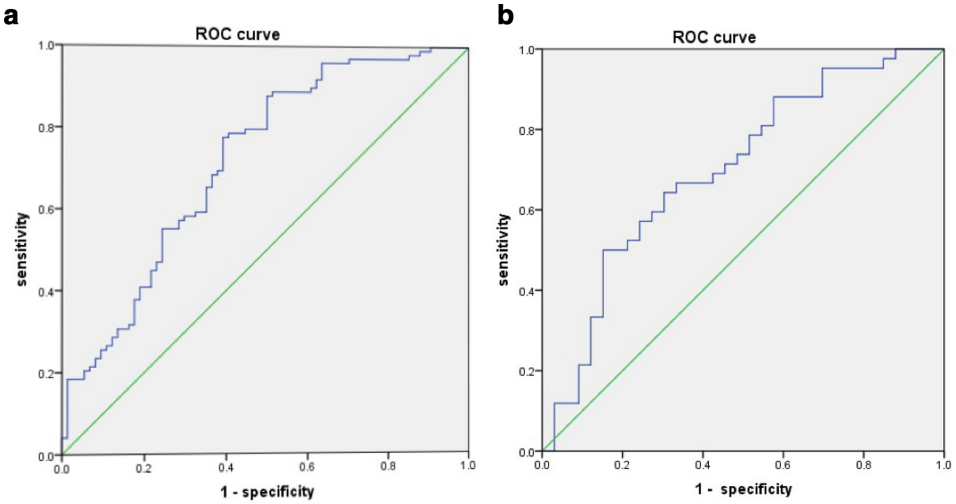

ml (with AUCs of 0.701–0.720). Our findings might have clinical implications for future clinical trials or practices, improving the ability to stratify the risk for HE or poor outcomes in patients with small hematomas. Because of the high density of hematomas relative to the surrounding edema or brain parenchyma, semi-automatic or automatic segmentation of hematomas may be applicable in the future, making it more convenient to apply radiomics.

There are some limitations in our study. First, it was a single-center retrospective study with a relatively small sample size. The small data set may influence the performance of the R-score in the training cohort and reduce the reliability of the verification in the test cohort. Further multicenter studies with larger samples are needed to support our findings. Second, the finding cannot be applied to all types of ICH due to the exclusion of patients with secondary ICH and anticoagulant treatment. Third, there was no lower limit of size when we evaluated patients with small ICH. Finally, the GOS score at discharge was the only prognostic indicator. Whether long-term neurological deterioration or mortality is associated with the R-score should be further investigated.

CONCLUSIONS

The addition of radiomic score to clinical factors can significantly improve the ability of discriminating between benign and malignant clinical course in patients with small ICH, particularly hematomas with a volume of 3–10 ml. Radiomics can be used as a supplement to conventional medical imaging, improving clinical decision-making and facilitating personalized treatment in ICH.

FUNDING

This work was supported by grants from the Fund of the Science and Technology Planning Projects of Wenzhou (grant no. Y20180112), the Health Foundation for Creative Talents in Zhejiang Province, China (grant no.: 2016), and the Project Foundation for the College Young and Middle-aged Academic Leader of Zhejiang Province, China (grant no.: 2017).

REFERENCES

1. van Asch CJ, Luitse MJ, Rinkel GJ, van der Tweel I, Algra A, Klijn CJ. Incidence, case fatality, and functional outcome of intracerebral haemorrhage over time, according to age, sex, and ethnic origin: a systematic review and meta-analysis. *Lancet Neurol* 2010; **9**: 167–76. doi: https://doi.org/10.1016/S1474-4422(09)70340-0
2. Al-Shahi Salman R, Frantzias J, Lee RJ, Lyden PD, Battey TWK, Ayres AM, et al. Absolute risk and predictors of the growth of acute spontaneous intracerebral haemorrhage: a systematic review and meta-analysis of individual patient data. *Lancet Neurol* 2018; **17**: 885–94. doi: https://doi.org/10.1016/S1474-4422(18)30253-9
3. Hemphill JC, Bonovich DC, Besmertis L, Manley GT, Johnston SC. The ICH score: a simple, reliable grading scale for intracerebral hemorrhage. *Stroke* 2001; **32**: 891–7. doi: https://doi.org/10.1161/01.str.32.4.891
4. Barras CD, Tress BM, Christensen S, MacGregor L, Collins M, Desmond PM, et al. Density and shape as CT predictors of intracerebral hemorrhage growth. *Stroke* 2009; **40**: 1325–31. doi: https://doi.org/10.1161/STROKEAHA.108.536888
5. Li Q, Yang W-S, Shen Y-Q, Xie X-F, Li R, Deng L, et al. Benign intracerebral hemorrhage: a population at low risk for hematoma growth and poor outcome. *J Am Heart Assoc* 2019; **8**: e011892. doi: https://doi.org/10.1161/JAHA.118.011892
6. Leasure AC, Sheth KN, Comeau M, Aldridge C, Worrall BB, Vashkevich A, et al. Identification and validation of hematoma volume cutoffs in spontaneous, supratentorial deep intracerebral hemorrhage. *Stroke* 2019; **50**: 2044–9. doi: https://doi.org/10.1161/STROKEAHA.118.023851
7. Nakagawa K, King SL, Seto TB. Optimal hematoma volume cut points to predict functional outcome after basal ganglia and thalamic hemorrhages. *Front Neurol* 2018; **9**: 291. doi: https://doi.org/10.3389/fneur.2018.00291

8. Ironside N, Chen C-J, Dreyer V, Christophe B, Buell TJ, Connolly ES. Location-Specific differences in hematoma volume predict outcomes in patients with spontaneous intracerebral hemorrhage. *Int J Stroke* 2020; **15**: 90–102. doi: https://doi.org/10.1177/1747493019830589
9. Qureshi AI, Palesch YY, Barsan WG, Hanley DF, Hsu CY, Martin RL, et al. Intensive blood-pressure lowering in patients with acute cerebral hemorrhage. *N Engl J Med* 2016; **375**: 1033–43. doi: https://doi.org/10.1056/NEJMoa1603460
10. Sprigg N, Flaherty K, Appleton JP, Al-Shahi Salman R, Bereczki D, Beridze M, et al. Tranexamic acid for hyperacute primary intracerebral haemorrhage (TICH-2): an international randomised, placebo-controlled, phase 3 superiority trial. *Lancet* 2018; **391**: 2107–15. doi: https://doi.org/10.1016/S0140-6736(18)31033-X
11. Delcourt C, Huang Y, Arima H, Chalmers J, Davis SM, Heeley EL, et al. Hematoma growth and outcomes in intracerebral hemorrhage: the INTERACT1 study. *Neurology* 2012; **79**: 314–9. doi: https://doi.org/10.1212/WNL.0b013e318260cbba
12. Dowlatshahi D, Smith EE, Flaherty ML, Ali M, Lyden P, Demchuk AM, et al. Small intracerebral haemorrhages are associated with less haematoma expansion and better outcomes. *Int J Stroke* 2011; **6**: 201–6. doi: https://doi.org/10.1111/j.1747-4949.2010.00563.x
13. Dowlatshahi D, Yogendrakumar V, Aviv RI, Rodriguez-Luna D, Molina CA, Silva Y, , et al. Small intracerebral hemorrhages have a low spot sign prevalence and are less likely to expand. *Int J Stroke* 2016; **11**: 191–7. doi: https://doi.org/10.1177/1747493015616635
14. Gillies RJ, Kinahan PE, Hricak H, , PE K. Radiomics: images are more than pictures, they are data. *Radiology* 2016; **278**: 563–77. doi: https://doi.org/10.1148/radiol.2015151169
15. Mayerhoefer ME, Materka A, Langs G, Häggström I, Szczypiński P, Gibbs P, et al. Introduction to Radiomics. *J Nucl Med* 2020; **61**: 488–95. doi: https://doi.org/10.2967/jnumed.118.222893
16. Chen T, Ning Z, Xu L, Feng X, Han S, Roth HR, et al. Radiomics nomogram for predicting the malignant potential of gastrointestinal stromal tumours preoperatively. *Eur Radiol* 2019; **29**: 1074–82. doi: https://doi.org/10.1007/s00330-018-5629-2
17. Nie P, Yang G, Wang Z, Yan L, Miao W, Hao D, et al. A CT-based radiomics nomogram for differentiation of renal angiomyolipoma without visible fat from homogeneous clear cell renal cell carcinoma. *Eur Radiol* 2020; **30**: 1274–84. doi: https://doi.org/10.1007/s00330-019-06427-x
18. Li H, Xie Y, Wang X, Chen F, Sun J, Jiang X. Radiomics features on non-contrast computed tomography predict early enlargement of spontaneous intracerebral hemorrhage. *Clin Neurol Neurosurg* 2019; **185**: 105491. doi: https://doi.org/10.1016/j.clineuro.2019.105491
19. Ma C, Zhang Y, Niyazi T, Wei J, Guocai G, Liu J, et al. Radiomics for predicting hematoma expansion in patients with hypertensive intraparenchymal hematomas. *Eur J Radiol* 2019; **115**: 10–15. doi: https://doi.org/10.1016/j.ejrad.2019.04.001
20. Shen Q, Shan Y, Hu Z, Chen W, Yang B, Han J, et al. Quantitative parameters of CT texture analysis as potential markersfor early prediction of spontaneous intracranial hemorrhage enlargement. *Eur Radiol* 2018; **28**: 4389–96. doi: https://doi.org/10.1007/s00330-018-5364-8
21. Dowlatshahi D, Demchuk AM, Flaherty ML, Ali M, Lyden PL, Smith EE, et al. Defining hematoma expansion in intracerebral hemorrhage: relationship with patient outcomes. *Neurology* 2011; **76**: 1238–44. doi: https://doi.org/10.1212/WNL.0b013e3182143317
22. Jiang J-Y, Xu W, Li W-P, Gao G-Y, Bao Y-H, Liang Y-M, et al. Effect of long-term mild hypothermia or short-term mild hypothermia on outcome of patients with severe traumatic brain injury. *J Cereb Blood Flow Metab* 2006; **26**: 771–6. doi: https://doi.org/10.1038/sj.jcbfm.9600253
23. Zuccarello M, Brott T, Derex L, Kothari R, Sauerbeck L, Tew J, et al. Early surgical treatment for supratentorial intracerebral hemorrhage: a randomized feasibility study. *Stroke* 1999; **30**: 1833–9. doi: https://doi.org/10.1161/01.str.30.9.1833
24. Rost NS, Smith EE, Chang Y, Snider RW, Chanderraj R, Schwab K, et al. Prediction of functional outcome in patients with primary intracerebral hemorrhage: the FUNC score. *Stroke* 2008; **39**: 2304–9. doi: https://doi.org/10.1161/STROKEAHA.107.512202
25. Broderick JP, Brott TG, Duldner JE, Tomsick T, Huster G. Volume of intracerebral hemorrhage. A powerful and easy-to-use predictor of 30-day mortality. *Stroke* 1993; **24**: 987–93. doi: https://doi.org/10.1161/01.STR.24.7.987
26. Wang X, Arima H, Al-Shahi Salman R, Woodward M, Heeley E, Stapf C, et al. Clinical prediction algorithm (brain) to determine risk of hematoma growth in acute intracerebral hemorrhage. *Stroke* 2015; **46**: 376–81. doi: https://doi.org/10.1161/STROKEAHA.114.006910
27. Wada R, Aviv RI, Fox AJ, Sahlas DJ, Gladstone DJ, Tomlinson G, et al. CT angiography "spot sign" predicts hematoma expansion in acute intracerebral hemorrhage. *Stroke* 2007; **38**: 1257–62. doi: https://doi.org/10.1161/01.STR.0000259633.59404.f3
28. Boulouis G, Morotti A, Charidimou A, Dowlatshahi D, Goldstein JN. Noncontrast computed tomography markers of intracerebral hemorrhage expansion. *Stroke* 2017; **48**: 1120–5. doi: https://doi.org/10.1161/STROKEAHA.116.015062
29. Morotti A, Boulouis G, Romero JM, Brouwers HB, Jessel MJ, Vashkevich A, et al. Blood pressure reduction and noncontrast CT markers of intracerebral hemorrhage expansion. *Neurology* 2017; **89**: 548–54. doi: https://doi.org/10.1212/WNL.0000000000004210
30. Morotti A, Brouwers HB, Romero JM, Jessel MJ, Vashkevich A, Schwab K, et al. Intensive blood pressure reduction and spot sign in intracerebral hemorrhage: a secondary analysis of a randomized clinical trial. *JAMA Neurol* 2017; **74**: 950–60. doi: https://doi.org/10.1001/jamaneurol.2017.1014
31. Liu Z, Wang S, Dong D, Wei J, Fang C, Zhou X, et al. The applications of Radiomics in precision diagnosis and treatment of oncology: opportunities and challenges. *Theranostics* 2019; **9**: 1303–22. doi: https://doi.org/10.7150/thno.30309
32. Xu W, Ding Z, Shan Y, Chen W, Feng Z, Pang P, et al. A nomogram model of Radiomics and satellite sign number as imaging predictor for intracranial hematoma expansion. *Front Neurosci* 2020; **14**: 491. doi: https://doi.org/10.3389/fnins.2020.00491
33. Chen Q, Zhu D, Liu J, Zhang M, Xu H, Xiang Y, et al. Clinical-radiomics nomogram for risk estimation of early hematoma expansion after acute intracerebral hemorrhage. *Acad Radiol* 2020;29 Mar 2020. doi: https://doi.org/10.1016/j.acra.2020.02.021
34. Rui W, Ren Y, Wang Y, Gao X, Xu X, Yao Z. MR textural analysis on T_2 FLAIR images for the prediction of true oligodendroglioma by the 2016 WHO genetic classification. *J Magn Reson Imaging* 2018; **48**: 74–83. doi: https://doi.org/10.1002/jmri.25896
35. Xie H, Ma S, Wang X, Zhang X. Noncontrast computer tomography-based radiomics model for predicting intracerebral hemorrhage expansion: preliminary findings and comparison with conventional radiological model. *Eur Radiol* 2020; **30**: 87–98. doi: https://doi.org/10.1007/s00330-019-06378-3